Chapter 4

Effect of Linker, Linkage, and Tail Modifications on Biological Activity of Pyrrole/Imidazole Polyamides

Abstract

Pyrrole/imidazole (Py/Im) hairpin polyamides are a class of small molecule DNA-minor groove binding compounds that have been shown to regulate endogenous gene expression *in vivo*. Gene regulation by polyamides requires efficient cellular uptake and nuclear localization properties for candidate compounds. To further optimize Py-Im polyamides for enhanced potency *in vivo*, a library of polyamides possessing various tail, linker and linkage moieties was synthesized and tested. Comparison of polyamide biological activity in two cell lines revealed tolerance for structural modifications and agreement in activity trends between cell lines. The use of an oxime linkage between the polyamide terminus and an aromatic functionality on the tail resulted in a ~20-fold increase in the potency of polyamides targeted to the Androgen Response Element (ARE) in LNCaP cells by measuring AR-activated PSA expression.

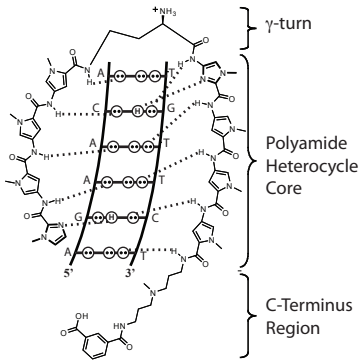

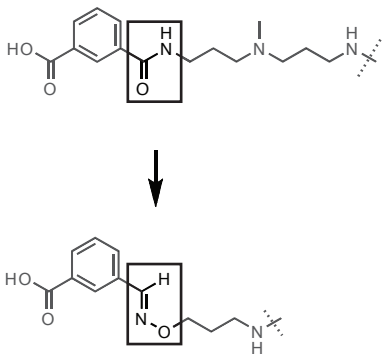

Introduction

Small molecules capable of regulating endogenous gene expression in a specific fashion could find numerous applications in molecular biology and human medicine.[1, 2] DNA-binding polyamides comprised of N-methylimidazole (Im) and N-methylpyrrole (Py) are a class of programmable small molecules that bind the minor groove of DNA in a sequence specific fashion and have been employed as regulators of gene expression through DNA-binding and modulation of the transcription factor-DNA interface.[3] Hairpin polyamides are comprised of two Im/Py strands linked via an aliphatic linker, with sequence specificity resulting in a programmed fashion from side-by-side heterocyclic amino acid pairings: Im/Py recognizes G•C over C•G; Py/Py is degenerate for A•T and T•A, while the 3-chlorothiophene N-terminus cap/Py recognizes T•A over A•T.[4-6] Eight-ring Im/Py polyamides have been shown to exhibit specific binding with binding affinities comparable to natural DNA-binding transcription factors.[7] Polyamide regulation of gene expression presumably occurs through either direct steric blockade of transcription factor binding sites or allosteric modification of DNA topology. While the sequence specificity and DNA-binding affinity of these small molecules is well studied, investigations into their potential therapeutic applications are active areas of investigation. We have recently shown that the biological activity of Im/Py polyamides can be improved via the incorporation of an isophthalic acid (IPA) group at the polyamide C-terminus, and we present here further structural modifications to polyamide tail and linker groups that increase even further their biological activity.[8]

Early *in vivo* gene regulation studies relied on fluorescein-polyamide conjugates as cell permeable compounds.[9-13] Subsequent studies in this arena aimed at eliminating the fluorescent tag utilized quantitative real-time RT-PCR to measure mRNA levels of an endogenous inducible gene as a biological readout of polyamide nuclear entry and DNA-binding. A focused library of minimized FITC analogues identified a stable, inexpensive replacement for fluorescein in the form of the IPA tail, which rivaled the activity of the

original FITC-labeled polyamide in HeLa (cervical cancer) and U251 (glioma) cells.[8] Subsequent work in other cell lines aimed at regulating different target genes has validated this C-terminus modification as a positive contributor to biological activity with negligible detrimental impact on polyamide sequence specificity or binding affinity.[14, 15]

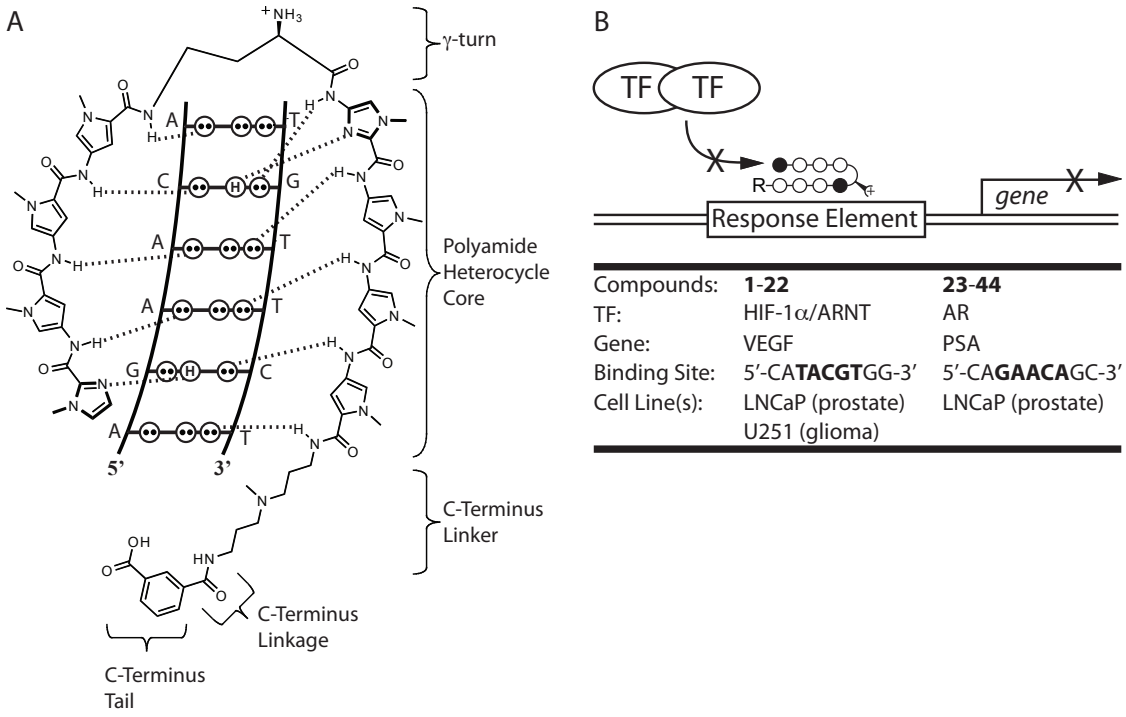

Figure 4.1. Project overview. A) Schematic illustration of polyamide-DNA recognition through formation of hydrogen bonds with the floor of the DNA minor groove. The γ-turn, polyamide heterocycle core, C-terminus linker, C-terminus linkage, and C-terminus tail of the polyamide are indicated by brackets and labeled for clarity. B) Schematic illustration of the mechanism by which polyamides affect gene expression. Sequence-specific binding of a polyamide core to a gene Response Element (RE) blocks Transcription Factor (TF) binding to the RE, thus blocking up-regulation of gene product expression under inducing conditions. Relative mRNA expression levels under inducing conditions were employed as a biological readout of polyamide cell uptake nuclear localization. Displayed in tabular form are the relevant transcription factors, gene products, DNA RE binding sequence, and cell lines for each set of match and mismatch polyamides.

The discovery of new moieties that facilitate polyamide cell uptake and nuclear localization for gene regulation studies is an area of keen interest as we aim to enhance further polyamide efficacy as we transition our studies towards animal disease models. The present study investigates the influence of linker, chemical linkage, and target cell line on polyamide nuclear localization utilizing a small library of C-terminus-modified polyamides (Figure 4.1). Quantitative real-time RT-PCR of relative mRNA expression levels in cells treated with polyamides was used as a measure of biological efficacy and the criterion for ranking

members of the polyamide library. Polyamides were targeted either to the vascular endothelial growth factor (VEGF) promoter in U251 (glioma) and LNCaP (prostate) cells, or to the prostate specific antigen (PSA) promoter in LNCaP cells (Figure 4.1B), as these two transcription-factor systems have been exploited for regulating such medically relevant genes by our group.[13-15] Although a variety of structural parameters were evaluated, it was discovered that a C-3 aliphatic linker tethered to an aromatic group through an oxime linkage resulted in enhanced polyamide potency. This motif has been employed recently by our group for the facile ^{18}F-labeling of polyamides for *in vivo* biodistribution by positron emission tomography.[16] This particular modification, as well as a variety of structural perturbations to the polyamide C-terminus, is discussed in detail.

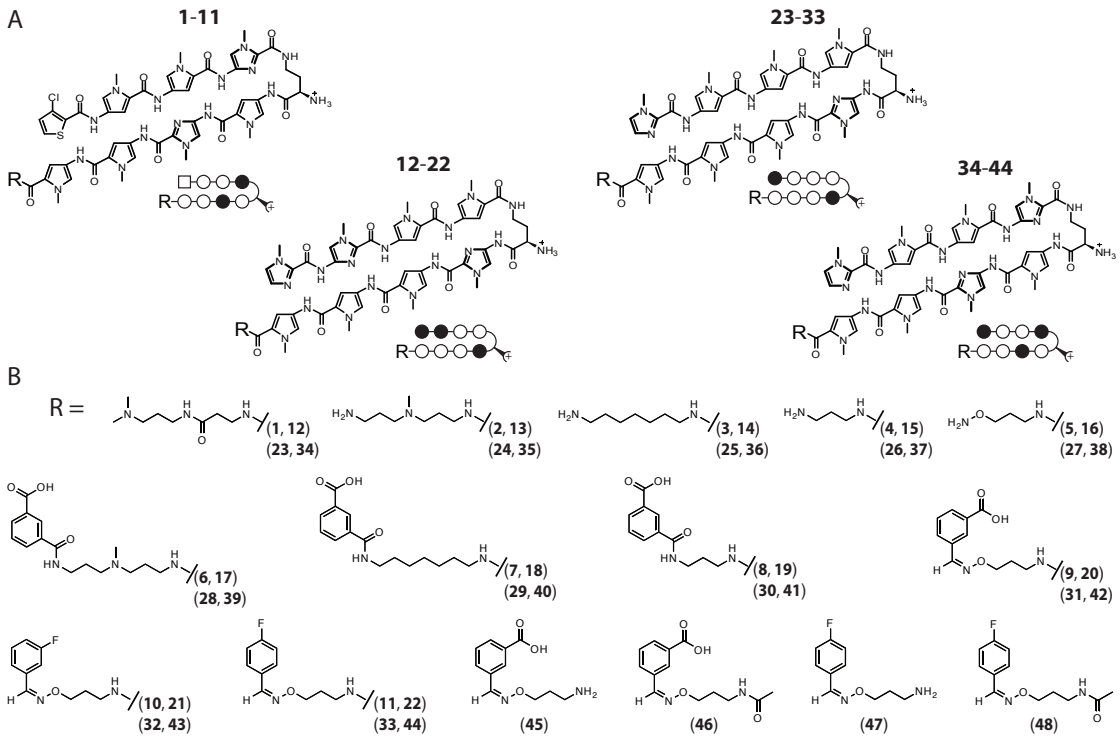

Figure 4.2. Schematic illustration of the polyamide cores and tail groups employed. A) At left are given the HRE match (**1**-**11**) and HRE mismatch (**12**-**22**) cores employed in U251 and LNCaP cells, and on the right the ARE match (**23**-**33**) and ARE mismatch (**34**-**44**) cores employed in LNCaP cells. Below the chemical structure is a schematic "ball-and-stick" shorthand representation of each core, in which pyrrole (Py) is symbolized by an open circle, imidazole (Im) by a filled circle, and chlorothiophene cap by an open square. B) The chemical structures of the tail groups "R" for compounds **1**-**44** are shown. Structures **45**-**48** are the "core-less" oxime-linked control compounds.

Results

Quantitative Real-Time RT-PCR data for Polyamide-Treated U251 and LNCaP cells

The biological activity against DFO-induced VEGF expression of HRE-targeted match (**6**-**11**) and mismatch (**12**-**22**) polyamides was studied in U251 and LNCaP cell culture, and of ARE-targeted match (**28**-**33**) and mismatch (**39**-**44**) polyamides against DHT-induced PSA expression in LNCaP cells. A schematic representation of polyamide-DNA binding and an overview of the project is shown in Figure 4.1, structures of the polyamide cores and tails are shown in Figure 4.2, and results for cell culture experiments in Figures 4.3-4.7. Polyamides that regulate VEGF expression under hypoxic (inducing) conditions target the hypoxia response element (HRE) 5'-A**TACGT**G-3' of the VEGF promoter (compounds **1**-**11**), and those that target PSA expression following dihydrotesterone (DHT) induction target the androgen response element (ARE) 5'-A**GAACA**G-3' of the PSA promoter (compounds **23**-**33**). For each gene, a set of mismatch control polyamides was included; mismatch polyamides are designed not to bind to the HRE or ARE, though some degree of biological activity is not unexpected, presumably due to off-target effects. The mismatch polyamides for the HRE series are **12**-**22** (target 5'-WGGWCW-3' sequences), and for the ARE series are **34**-**44** (target 5'-WGWCGW-3' sequences). These compounds are linked either through an amide linkage (**6**-**8**, **17**-**19**, **28**-**30** and **39**-**41**) or an oxime linkage (**9**-**11** and **20**-**22, 31**-**33** and **42**-**44**) to a C-terminal tail group. For each linker group, unconjugated free amine control compounds lacking a tail moiety (**2**-**5** and **13**-**16**, **24**-**27** and **35**-**38** (match and mismatch polyamides, respectively)) were included: due to its historical use and known modest level of biological activity, βDp tail (**1**, **12, 23** and **34**) polyamides were included for further comparison. Polyamide-untreated uninduced and polyamide-untreated induced conditions were used as controls, and VEGF or PSA mRNA expression levels in treated cells were normalized to those in the untreated, induced controls. Induced and uninduced DMSO-treated control conditions were included to rule out vehicle (DMSO) as the source of relative mRNA expression changes (DMSO concentration ≤ 0.1% for all biological

experiments)[17]. Unless otherwise noted, U251 cells were dosed with polyamides at 1, 0.2 and 0.02 μM, and LNCaP cells were dosed at 10, 2 and 0.2 μM; for both the VEGF and PSA systems, cells were dosed with control unconjugated control polyamides only at the highest concentration.

Biological Activity of HRE-targeted polyamides in U251 and LNCaP cells The data obtained for the amide-linked HRE series in U251 and LNCaP are shown in Figures 4.3A and 3B, respectively. The biological activity measured for **6** is comparable to previously obtained data for **6** at 1 μM in U251 cells.[8, 15] The general trend in this cell line indicates that the unconjugated control compounds lacking the IPA tail moiety all exhibited a modest degree of activity, but that activity is improved through IPA conjugation. IPA conjugation resulted in a greater increase in activity for compounds bearing the triamine linker than for compounds bearing the C7-linker or C3-linker. The βDp tail was the least active of all tails in this series. In LNCaP cells, the unconjugated controls were more active than in U251 cells, with the unconjugated parent compound **4** as active as IPA conjugates **6**-**8**. Conjugation of the IPA tail increased the activity of the triamine and C7-linked compounds, but the difference in activity between unconjugated parents and the IPA derivatives was more modest than in U251 cells. The βDp tail polyamides (**1** and **12**) were more active in LNCaP than U251.

The activity of the HRE oxime-linked series was measured in U251 and LNCaP, and the results are shown in Figure 4.6A and 4.6B, respectively. Compounds **9**-**11** were active in U251 cells under hypoxic conditions: VEGF mRNA expression was downregulated ~60% in U251 cells treated with 1 μM **9**-**11**, which is comparable to the activity of **6** at 1μM in U251 (Figure 4.3A). Mismatch polyamide compounds **20**-**22** were as active in U251 cells as their respective match polyamides **9**-**11.** In LNCaP cells, compounds **9**-**11** were also active: VEGF mRNA expression levels measured for cells treated with 10 μM **9**-**11** were downregulated ~80%. Mismatch oxime-linked polyamides were significantly active in LNCaP cells.

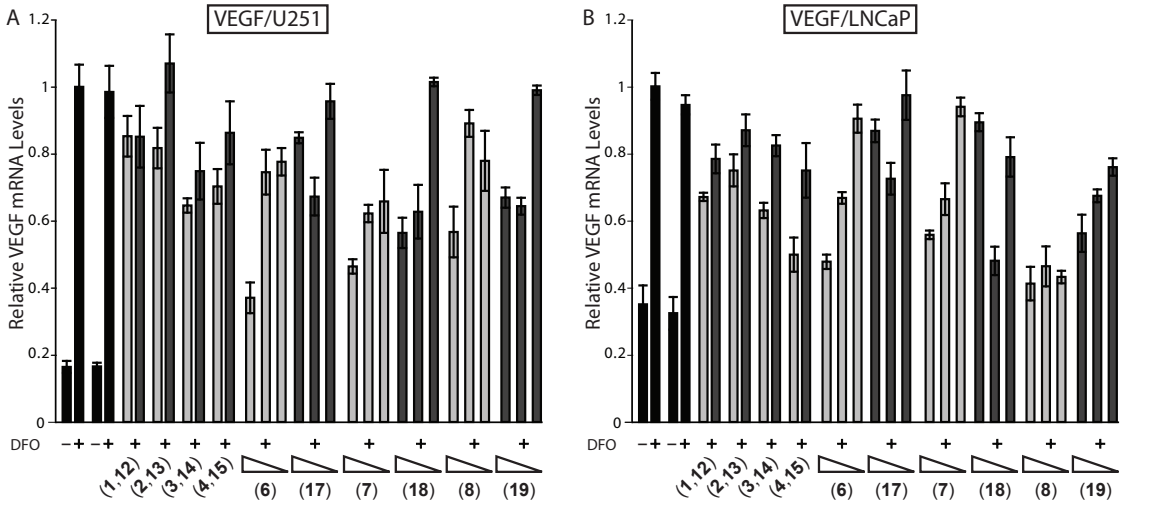

Figure 4.3. Quantitative real-time RT-PCR data showing the effect of HRE-targeted match compounds **1**-**4**, **6**-**8** and their mismatch congeners **12**-**15**, **17**-**19** on DFO-induced VEGF expression in cultured cells. Induced and uniduced control conditions are indicated by black bars, match core compounds by light grey bars, and mismatch core compounds by dark grey bars. Uninduced and induced control compounds without DMSO are on the left, and with 0.1% DMSO on the right. Errors shown are the fractional standard deviation. A) Expression of VEGF in cultured **U251** cells under DFO-induced hypoxic conditions of match core control compounds **1**-**4** and mismatch core control compounds **12**-**15** at 1 μM concentration. Cells were treated with match compounds **6**-**8** and respective mismatch compounds **17**-**19** as 1, 0.2 and 0.02 μM cell culture media solutions. B) Expression of VEGF in cultured **LNCaP** cells under DFO-induced hypoxic conditions of match core control compounds **1**-**4** and mismatch core control compounds **12**-**15** at 10 μM. Cells were treated with match compounds **6**-**8** and respective mismatch compounds **17**-**19** as 10, 2 and 0.2 μM cell culture media solutions.

Biological Activity of ARE-targeted polyamides in LNCaP cells The relative PSA mRNA levels in LNCaP cells induced with 1 nM DHT and dosed with polyamides **23**-**44** were measured (Figure 4.4 and Figure 4.6C.) In the amide series, the unconjugated free amine control compounds **23**-**26** were more active than mismatch controls **34**-**37**. Amide-linked ARE compounds **28**-**30** were appreciably active, and a modest linker effect was observed (C7 > C3 > triamine); mismatch compounds **39**-**41** were less active than their match mates. The difference in activity between each match **28**-**30** and respective mismatch **39**-**41** was greater than measured for VEGF regulation in U251 and LNCaP cells.

The activity of the oxime-linked series **31**-**33** and **42**-**44** in LNCaP cells was measured at 5, 1 and 0.1 μM and unconjugated controls **27** and **38** at 5 μM; the data are shown in Figure 4.6C. A significant increase in biological activity was measured for match polyamides **31**-**33**: all three compounds decreased PSA mRNA levels at 5 μM below untreated, uninduced levels. PSA mRNA levels were reduced to untreated, uninduced levels at 1 μM **31** and **33.**

Mismatch polyamides **42**-**44** were less active than their respective match polyamides **31**-**33**. The hydroxylamine match control compound **27** downregulated PSA mRNA levels by ~50%, while the hydroxylamine mismatch compound **38** showed very little activity. LNCaP cells treated with 5 μM **31**-**33** showed noticeable cytotoxic response upon incubation for 48 hours, an effect that was more pronounced for **32** and **33** as compared to **31**.

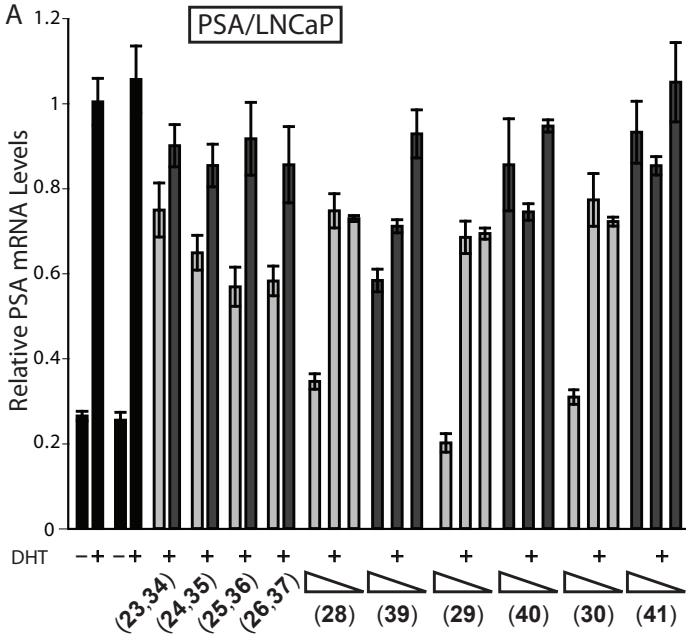

Figure 4.4. Quantitative real-time RT-PCR data measuring the effect on relative PSA mRNA expression levels under DHT induction in **LNCaP** cells dosed with compounds **23**-**26**, **28**-**30** and their mismatch congeners **34**-**37** and **39**-**41**. Induced and uniduced control conditions are indicated by black bars, match core compounds by light grey bars, and mismatch core compounds by dark grey bars. Uninduced and induced control compounds without DMSO are on the left, and with 0.1% DMSO on the right. Errors shown are the fractional standard deviation. Cells were treated with match core control compounds **23**-**26** and mismatch core control compounds **34**-**37** as cell media solutions 5 μM in polyamide. Cells were treated with match compounds **28**-**30** and respective mismatch compounds **39**-**41** as 5, 1, and 0.1 μM solutions in cell culture media.

DNA Melting Temperature (Tm) The effect of polyamide binding on 14-mer oligonucleotide melting temperature (Tm) was measured (Table SI 2) to determine whether differences in biological activity by quantitative real-time RT-PCR correlate to differences in binding affinities.[18] Tm measurements require minimal materials and present a rapid method for determining the rank-order of binding affinities, although a quantitative K_a value is not obtained. The 14-mer oligonucleotide sequences (Materials and Methods) are based on the HRE of VEGF and ARE of PSA, respectively. For both the HRE and ARE 14-mers, the melting temperature increased appreciably upon match compound binding (**1**-**11**

and **23**-**33**, respectively). Tms also generally increased upon mismatch binding (**12**-**22** and **34**-**44**, respectively), but to a more modest degree. Melting temperatures of the free amine parent compounds were higher than those of the IPA conjugates, with the exception of **36** versus **40**. The ΔTm values calculated for match and mismatch compounds ranged from a 0.1°C to 14.8°C increase for the HRE polyamide series, and from a -0.9°C drop to 17.3°C increase for the ARE series.

Table 4.1. Melting temperatures and ΔTm values measured for **1**-**44** on 14-mer oligonucleotides containing the HRE or ARE sequences (oligonucleotide sequences in Materials and Methods). All values reported are averages of at least three melting temperature experiments (standard deviations indicated in parentheses.)

	5′-G T G C **A T A C G T** G G G C-3′ 3′-C A C G **T A T G C A** C C C G-5′			5′-T T G C **A G A A C A** G C A A-3′ 3′-A A C G **T C T T G T** C G T T-5′	
Compound Number	Tm (°C)	ΔTm (°C)	**Compound Number**	Tm (°C)	ΔTm (°C)
DNA Only	64.7 +/- 0.2		**DNA Only**	60.8 +/- 0.2	
1	77.1 +/- 0.2	12.3	**23**	75.1 +/- 0.3	14.3
2	79.5 +/- 0.2	14.7	**24**	78.1 +/- 0.2	17.3
3	77.4 +/- 0.2	12.7	**25**	75.1 +/- 0.2	14.3
4	78.2 +/- 0.2	13.5	**26**	77.0 +/- 0.2	16.2
5	75.3 +/- 0.1	10.6	**27**	72.0 +/- 0.3	11.2
6	76.4 +/- 0.2	11.7	**28**	73.6 +/- 0.1	12.8
7	73.7+/- 0.0	9.0	**29**	71.2 +/- 0.2	10.4
8	74.2 +/- 0.2	9.5	**30**	71.9 +/- 0.2	11.1
9	76.1 +/- 0.2	11.4	**31**	72.3 +/- 0.2	11.5
10	74.1 +/- 0.2	9.4	**32**	73.3 +/- 0.1	12.5
11	75.2+/- 0.2	10.5	**33**	73.7 +/- 0.3	12.9
12	66.3 +/- 0.2	1.6	**34**	64.4 +/- 0.2	3.6
13	67.8 +/- 0.2	3.1	**35**	67.2 +/- 0.1	6.4
14	66.8 +/- 0.2	2.1	**36**	59.9 +/- 0.2	-0.9
15	68.9 +/- 0.0	4.1	**37**	66.1 +/- 0.2	5.3
16	64.8 +/- 0.2	0.1	**38**	62.8 +/- 0.2	2.0
17	65.6 +/- 0.2	0.9	**39**	64.0 +/- 0.2	3.2
18	65.4 +/- 0.2	0.7	**40**	63.4 +/- 0.2	2.6
19	65.2 +/- 0.2	0.5	**41**	62.3 +/- 0.2	1.5
20	65.6 +/- 0.3	0.8	**42**	63.4 +/- 0.0	2.6
21	65.7 +/- 0.2	0.9	**43**	64.8 +/- 0.1	4.0
22	65.5 +/- 0.2	0.8	**44**	64.2 +/- 0.2	3.4

ΔTm = Tm(DNA+polyamide) – Tm(DNA only).

Cell Viability Effects of ARE-targeted match compounds 28-33 and 39-44 in LNCaP cells LNCaP cells were dosed with each compound at concentrations spanning 30 to 0.01 μM, and metabolic activity measured with a standard WST-1 colorimetric assay. Metabolic activity decreased with increasing concentrations of **28**-**30**, but did not significantly surpass 50% viability; therefore IC_{50} values for growth inhibition could not be calculated. Cells treated with the mismatch mates (**39**-**41**) had little effect on cell growth. The three oxime-linked match compounds had measurable IC_{50} values for growth inhibition: **31** = 1.7 ± (0.3) μM, **32** = 0.6 ± (0.1) μM, and **33** =0.4 ± (0.0) μM. The mismatch oximes displayed a similar pattern; the growth inhibition of the fluorine-bearing oximes **43** and **44** was more pronounced than the 3-carboxy tail mismatch **42**, but the effect on cell growth of the mismatch polyamides was less pronounced than that of the match polyamides. The cell growth data for **28**-**33** and **39**-**44** in LNCaP are shown in Figure 4.6 and Table 4.2.

Cell Viability Effects of Control compounds 45-48 in U251 and LNCaP cells IC_{50} values for growth inhibition in U251 cells treated with oxime-linked polyamide core-less compounds **45**-**48** at a range of 10–0.002 μM and LNCaP cells at 50–0.02 μM were measured by a standard WST-1 colorimetric assay. Negligible cell viability effects were measured in either U251 or LNCaP cells after a 48-hour treatment course with **45**-**48** at the concentrations used. These data are shown in Figure 4.5.

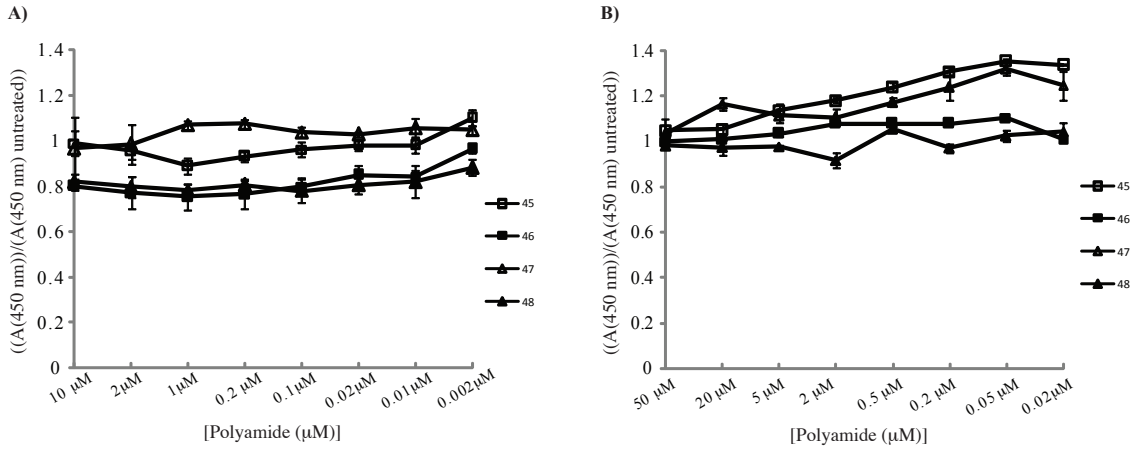

Figure 4.5. Cell viability data for **45**-**48** in U251 and LNCaP cells, performed according to the protocol provided in main text. A) Cell viability data for **45**-**48** in U251 cells at 10, 2, 1, 0.2, 0.1, 0.02, 0.01 and 0.002 μM. B) Cell viability data for **45**-**48** in LNCaP cells at 50, 20, 5, 2, 0.5, 0.2, 0.05 and 0.02 μM.

Gene Regulation IC_{50} Values for ARE-targeted oxime-linked compounds in LNCaP cells IC_{50} values for PSA mRNA expression levels were measured for **28**, **31** and **33** by quantitative real-time RT-PCR in LNCaP cells; **28** was used as a benchmark, and **31** and **33** were selected on the basis of their high biological activity and to provide variety in the tail substitution. Cells were dosed with **28** at a range of 30–0.1 μM and **31** and **33** at 10–0.03 μM. Isotherms were generated for each of three independently performed real-time quantitative RT-PCR experiments in LNCaP cells for **28**, **31** and **33**. An IC_{50} value was generated for each run, and the IC_{50} value given in Table 4.1 for each compound is the average value of three independent measurements (error given is the standard error of the mean (SEM) between the three independent runs). Isotherms (Figure 4.7B) were generated from the average value of the independent runs at each concentration (error bars are the SEM for each data point). Average IC_{50} values for gene regulation were as follows: **28** = 6.0 (± 2.6) μM, **31** = 0.28 (± 0.1) μM, and **33** = 0.6 (± 0.3) μM.

Discussion

A focused library of polyamides was synthesized with different modifications at the C-terminus, in which the linker, linkage and tail group were varied and tested in two separate cell lines for gene regulation activity of two different target genes. Prior to the current study, no direct comparison of the gene regulatory activity of a polyamide series between multiple cell lines had been performed. Measurement of VEGF mRNA expression levels in both U251 and LNCaP for the entire amide- and oxime-linked series was performed in an effort to evaluate whether modifications in tail or linker structures can have differing effects on biological activity in a cell-line dependent fashion. The polyamide dose required to effect gene regulation activity was found to be cell-line dependent, but the trend in relative activities of polyamides did not vary greatly between different cell lines. Two encouraging results of this study were the degree to which changes in the linker composition are well tolerated, and the significant increase in biological activity achieved upon replacement of an amide linkage with an oxime linkage between the linker and tail groups.

The biological activity of a series of polyamides targeted to the HRE of VEGF was measured under hypoxic (inducing) conditions in two different cell lines, U251 (glioma) and LNCaP (prostate cancer) lines. Polyamide regulation of DFO-induced VEGF expression in LNCaP cells has not previously been published. In the HRE-targeted amine series (**1**-**8** and **12**-**19**), a slight linker effect was observed, but varied between the two cell lines. Overall, changes in the linker group did not dramatically affect biological activity in either cell line. The most pronounced effect was conjugation of the IPA tail, which resulted in an increase for each linker group in both cell lines, with the exception of the C3 linker in LNCaP cells. IPA conjugation affected biological activity of the triamine-linked compounds most significantly in both U251 and LNCaP.

The amide-linked ARE series was assayed for activity against DHT-induced, AR-regulated PSA expression in LNCaP cells. Removal of the tertiary amine in the linker resulted in an increase in biological activity, as seen for **29** vs. **28**, while reduction in linker length from a C7 to a C3 linker led to a modest loss of activity (**29** vs. **30**). Although the mechanism by which mismatch polyamides affect gene expression is unknown, removal of the tertiary amine reduces mismatch activity (e.g. **39** is more active that **40** and **41**); it has previously been observed by DNase I titration footprint experiments that polyamides bearing multiple positive charges bind nonspecifically to DNA, and it may be here that the presence of the positive charge reduces the off-rate of DNA-bound polyamide and results in less specific binding compared to a charge-neutral compound. These results again indicate that there is tolerance of linker group modification, and that the ARE system in LNCaP cells benefits from removal of the amine group in the linker. The Tm data indicate that the absence of biological activity is not due to an inability of the polyamides to bind to DNA, as each of the IPA conjugates has a lower Tm than their respective free-amine parent compounds, but higher biological activity. The triamine-bearing polyamides **24** and **28**, in fact, have higher Tm values than the neutral, aliphatic linker-bearing polyamides **25** and **29** (C7 linker) and **26** and **30** (C3 linker) (free amine and IPA, respectively, for each pair). These data suggest

that the presence of the tertiary amine and the potential positive charge increase the binding affinity of these polyamides. The potential downside of the positive charge, however, is abrogation of binding specificity, presumably due to a slower polyamide off-rate, which would increase the chances of the polyamide binding to sites other than the designed target sequence. As this is not the same trend observed for the HRE series in U251 and LNCaP cells, it is difficult to be certain in absence of a quantitative study of polyamide nuclear concentration as a function of linker modifications.

Oxime-linked polyamides were synthesized for both the HRE (**9**-**11**, **20**-**22**) and ARE (**31**-**33**, **42**-**44**) systems. The oxime had been introduced as an efficient means of conjugating a polyamide core to ^{18}F-labeled 4-fluorobenzaldehyde for PET studies, but the ability of polyamides possessing this motif to regulate endogenous gene expression was not known. The aldehyde tail groups selected were 4-fluorobenzaldehyde, 3-fluorobenzaldehyde and 3-carboxybenzaldehyde; 3-fluorobenzaldehyde was selected to probe position effects, and 3-carboxybenzaldehyde provided an oxime-linked mimic of the amide-linked IPA tail.

In U251 cells (Figure 4.6A), the oxime linked match (**9**-**11**) polyamides had activity comparable to the triamine- or C7-linker amide-linked IPA conjugates (**6** and **7**, respectively). Introduction of the oxime linker had a more significant impact on the biological activity of the mismatch polyamides **20**-**22**, which were as active as their oxime-linked counterparts **9**-**11**. A similar result was seen for the C7- and C3-linker, amide-linked IPA conjugate pairs **7** and **18**, and **8** and **19**, in U251 cells. Thus, although there does appear to be tolerance of linker variations, the greatest difference in biological activity within an HRE match-mismatch pair in U251 cells is the triamine-linked IPA compounds **6** and **17**.

In LNCaP cells (Figure 4.6B), the HRE-oxime series **9**-**11** were more active than the amide-linked series **6**-**8**, and in fact reduced VEGF mRNA expression levels to below baseline levels. In this case, introduction of fluorine on the tail restored the match-mismatch activity difference to ~two-fold (i.e. **9** and **20**, or **10** and **21**, or **11** and **22**). The Tm data for the oxime-linked polyamides and their parent unconjugated polyamides do not indicate that

differences in binding affinity play any role in the differences in activity; the Tm values measured for the amide series, both match and mismatch cores, are comparable to those measured for the oxime series.

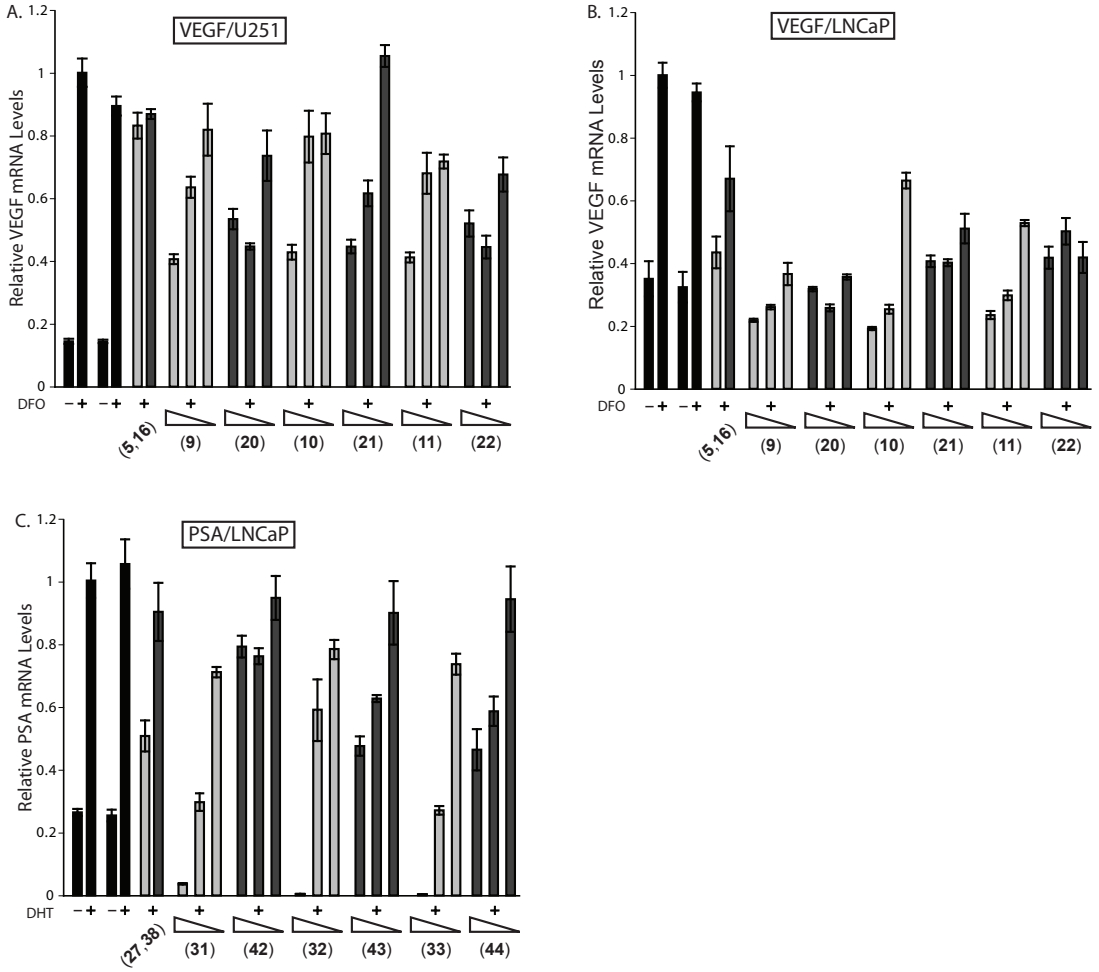

Figure 4.6. Gene-regulation effects measured by quantitative real-time RT-PCR for the oxime-linked polyamides **9**-**11**, **20**-**23**, **31**-**33** and **42**-**44**, and the hydroxylamine tail control compounds **5**, **16**, **27**, and **38**. Induced and uniduced control conditions are indicated by black bars, match core compounds by light grey bars, and mismatch core compounds by dark grey bars. Uninduced and induced control compounds without DMSO are on the left, and with 0.1% DMSO on the right. Errors shown are the fractional standard deviation. A) Effect on DFO-induced expression of VEGF by HRE-targeted match and mismatch polyamide cores in **U251** cells at 1, 0.2, and 0.02 μM; B) Effect on DFO-induced expression of VEGF by HRE-targeted match and mismatch polyamide cores in **LNCaP** cells at 10, 2 and 1 μM; C) Effect on DHT-induced expression of PSA mRNA by ARE-targeted match and mismatch polyamide cores in **LNCaP** cells at 5, 1 and 0.1 μM.

Polyamide regulation of VEGF expression in LNCaP had not been studied, but it was known that polyamide-effected regulation of PSA in LNCaP cells can be achieved with 10 and 5 μM **28**. A ten-fold higher concentration of HRE polyamides was required in LNCaP cells as compared to U251 cells to effect comparable VEGF gene regulation. Although the effects on VEGF expression in LNCaP and U251 cells of the HRE polyamide series

vary somewhat, it is encouraging that there are no drastic difference in biological activity measured for any of the compounds tested between the two cell lines. This suggests that a structural modification that results in increased gene regulation in one cell line may have a similar effect for the same core in other cell lines.

The data for the oxime-linked ARE series (**31**-**33**, **42**-**44**) in LNCaP cells (Figure 4.6C) indicate that the oxime linkage greatly increases the gene regulation activity of the ARE polyamides. PSA mRNA expression was negligible in cells treated with **31**-**33** at 5 μM, but there was evidence of cell death upon visual inspection (vide infra) and levels of total mRNA were very low. The average gene expression titration curve generated by quantitative real-time RT-PCR for **28**, **31** and **33** is shown in Figure 4.7B. These data illustrate the impact of the oxime linkage on the biological activity, as the activity curves of the oxime compounds **31** and **33** are shifted down by a factor of ≥10-fold from the amide-linked triamine IPA parent polyamide **28** (IC_{50} values in Table 4.1).

Table 4.2. Table of IC_{50} values (μM) for Growth Inhibition and Gene Regulation in LNCaP cells for **28**-**33**; data is shown in Figure 4.6. IC_{50} for gene regulation was measured only for **28**, **31** and **33**. For **28**, **31** and **33**, the (IC_{50} for Growth Inhibition)/(IC_{50} for Gene Regulation) ratio was calculated.

Compound Number	Growth Inhibition IC50 (μM)	Gene Regulation IC50 (μM)	Growth Inhibition IC50 (μM) / Gene Regulation IC50 (μM)
28	> 30	6.0 (+/- 2.6)	≥5
29	> 30	------	
30	> 30	------	
31	1.7 (+/- 0.3)	0.3 (+/- 0.1)	6.1
32	0.6 (+/- 0.1)	------	
33	0.4 (+/- 0.0)	0.6 (+/- 0.3)	0.7

To quantitate the effect of **28**-**33** and **39**-**44** on cell growth in LNCaP cells, cells were treated with compounds and viability was measured (Figure 4.7A **(28**-**33**) and 4.7C (**39**-**44**)). Cells treated with the amide-linked compounds at these concentrations did not show ≥50% decrease in cell growth, so an IC_{50} value for growth inhibition could not be calculated. IC_{50} values for growth inhibition were calculated for **31**-**33** (Table 4.1.) Oxime mismatch polyamide **42** minimally affected cell viability, while **43** and **44** had estimated IC_{50} values for cell viability are ≥ 30 μM**.** The IC_{50} values for gene regulation for **31** and **33** are 20- and

10-fold lower than **28**, respectively. In the case of the 4-Fluoro oxime-linked compound **33**, the IC_{50} for growth inhibition and for gene regulation are within error of each other. The IC_{50} for growth inhibition of **28** and **31** is ~5-fold higher than the IC_{50} values for gene regulation, but both these values are ~20-fold lower for **31** that **28**, indicating that **31** is ~20-fold more potent than **28** and more specific than **33**.

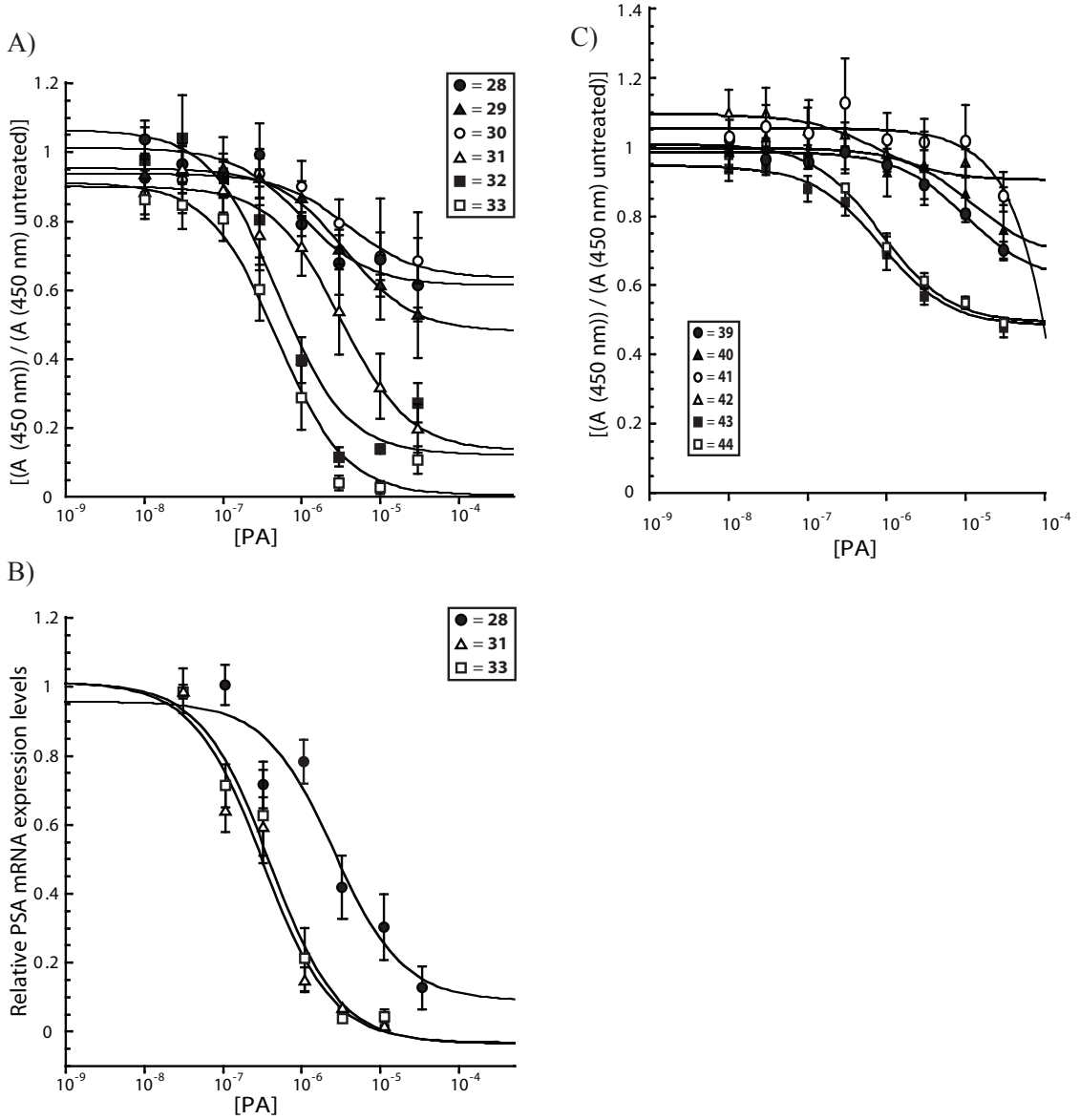

Figure 4.7. Cell viability data and IC_{50} values for gene regulation for in **LNCaP** cell culture. A) Cell viability was measured by a WST-1 colorimetric assay for **LNCaP** cells dosed for 48 hours with polyamides **28-33** at the following concentrations: 30, 10, 3, 1, 0.3, 0.1, 0.03 and 0.01 μM. For **31-33**, IC_{50} values for cell viability were extracted from isotherms generated in KaleidaGraph from the data. B) Quantitative real-time RT-PCR data for **28**, **31** and **33** in **LNCaP** cells to establish IC_{50} values for PSA gene regulation under inducing conditions. Concentrations employed of **28** were 30, 10, 3, 1, 0.3 and 0.1 μM, and of **31** and **33** were 10, 3, 1, 0.3, 0.1 and 0.03 μM. IC_{50} values were extracted from isotherms generated in Kaleidagraph from the RT-PCR titrations. C) IC_{50} values (μM) for cell viability estimated or calculated for **28-33** and IC_{50} values (μM) for PSA gene regulation for **28**, **31** and **33** shown in tabular format. Values given are average values of three independent experiments; the standard error of the mean is given in parentheses.

These results indicate that the oxime linkage can effect a significant increase in the cell uptake and gene regulation activity of polyamides. For unconjugated hydroxylamine polyamides **27** and **38**, a ~50% and 10% downregulation was measured, respectively, of induced PSA mRNA expression in LNCaP cells at 5 μM, and **27** and **38** were significantly less active than the oxime conjugates. Although previous studies have rigorously verified the stability of oxime-linked conjugates *in vivo*, a control experiment employing polyamide-lacking compounds **45**-**48** were synthesized and their cytotoxicity measured.[19] It was rationalized that equivalent cytotoxicity to oxime polyamide conjugates would serve as an indirect measure of bond lability, whereas a lack to toxicity would reinforce the robustness of this chemical bond. The growth inhibitory effects of these compounds were studied in U251 and LNCaP cells (Figure 4.6). Treatment with **45**-**48** in both cells lines failed to cause dramatic cell death at any concentrations used (10–0.002 μM in U251, 50–0.02 μM in LNCaP), indicating that the oxime linkage did not decompose and invoke cell death. These results suggest that the oxime-linkage is promising for future work aimed at increasing polyamide potency.

Although not the focus of the current study, the mechanism(s) of polyamide cell entry, nuclear localization and cell exit are active areas of investigation.[11] Our current working hypothesis for polyamide biological activity is that passive or non-specific mechanisms of polyamide cell uptake and competing efflux pathways influence polyamide accumulation in the cell nucleus, and structural modifications that result in improved polyamide biological activity may reflect a decrease in efflux. Polyamides are believed in part to undergo active efflux by p-glycoprotein pumps, which have more pronounced activity in immortalized cancer cells such as those employed in the current study.[20,21] The chemical agent verapamil, which inhibits p-glycoprotein pump activity, has been found to result in nuclear localization for some fluorophore-polyamide conjugates.[10] The mechanistic basis for the improved activity observed upon introduction of structural features such as the IPA tail is unknown, but we speculate that it is partially due to reduced polyamide efflux.

The tolerance of modifications to the linker group suggest that further modifications to the linker group may lead to improved polyamide biological activity. Comparison of the data gathered for the HRE match and mismatch polyamides in U251 and LNCaP cells indicate that, while the concentrations required to achieve acceptable levels of gene regulation activity will vary between cell lines, the effect of structural modifications will most likely be comparable between cell lines, i.e. the trends in activity will translate between cell lines. In addition, the use of an oxime linkage in place of an amide linkage between the tail and linker groups was found to increase the gene regulation activity of polyamides. This increase was most noticeable for the ARE oxime-linked series **31**-**33** in LNCaP cells. The dramatic increase in activity measured for **31** compared to the previously published **28** makes this compound and related derivatives useful for future ARE studies. In addition, these results suggest that the oxime linkage may be a useful structural feature to increase the biological activity of polyamides in other biological studies. Although this study did not uncover a set of predictive structural requirements for polyamide cell uptake, the discovery of the utility of the oxime linkage for gene regulation studies is a welcome addition to the known set of structural modifications to increase polyamide cell uptake.

Materials and Methods

Synthesis of Polyamides. Polyamides were synthesized by solid-phase methods on Kaiser oxime resin (NovaBiochem), or Boc-β-alanine-PAM resin (Peptides International), were cleaved from resin with 3,3'-diamino-*N*-methyl-dipropylamine, N, N'-dimethylpropane-1, 3-diamine (Dp), heptane-1, 7-diamine, propane-1, 3-diamine or *tert*-butyl 3-aminopropoxycarbamate, and purified by reverse-phase HPLC.[16, 22-24] Synthesis of IPA conjugates and oxime conjugates was as previously described.[8, 16] Reaction progress was monitored by analytical HPLC at 310 nm. Turn deprotection was done through addition of 1 mL 1:1 TFA:DCM at ambient temperature, and purification by reverse-phase preparatory HPLC performed immediately following successful deprotection. Reverse-phase HPLC solvent systems were 0.1% TFA (aqueous) and acetonitrile. Polyamide purity and identity

were assessed by analytical HPLC and MALDI-ToF MS, and polyamides quantitated by UV-vis at 310 nm (ε = 69,360 M^{-1} cm^{-1} for eight-ring hairpin polyamides). All polyamides were ≥95% by analytical HPLC (310 nm). Supporting Information Table SI 1 provides expected and observed ($M+H^+$) (MALDI-ToF), and purity by analytical HPLC for **1**-**44**. ^1H and ^{13}C NMR spectra were obtained on a 500 MHz spectrometer.

Synthesis of 45. 1 equivalent (84.3 mg, 0.44 mmol) of *tert*-butyl 3-(aminooxy) propylcarbamate was dissolved in 300 μL DMF, and 1.2 equivalents of 3-formyl benzoic acid added as a 50 mM solution in DMF.[25] Reaction progress was monitored by analytical HPLC at 254 nm for starting material consumption and production of a mixture of the E and Z -3-(10,10-dimethyl-8-oxo-3,9-dioxa-2,7-diazaundec-1-enyl)benzoic acid intermediate. Upon consumption of starting material, the Boc protecting group was removed by addition of 4 mL of 1:1 TFA:DCM. After 15 minutes, the reaction was concentrated by rotovap, and the product purified by reverse phase preparatory HPLC. The E and Z products were separable by preparatory HPLC, but interconvert at room temperature on the time scale of the experiments, so were recombined to yield 43.3 mg (44% yield) of 3-((3-aminopropoxyimino)methyl)benzoic acid (**45**). ^1H NMR (DMSO-d_6): δ 13.23 (s, 1H), 8.36 (s, 1H), 8.20 (app t, J = 1.8 Hz, 1H), 7.96 (app dt, 7.8, 1.8, 1 Hz, 1H), 7.88 (br s, 3H), 7.84 (app dt, 8.0, 1.5 Hz, 1H), 7.55 (app t, 7.8 Hz, 1H), 4.20 (t, 6.3 Hz, 2H), 2.91 (t, 7.3 Hz, 2H), 1.96 (m, 2H). ^{13}C NMR (DMSO-d_6): δ 166.8, 148.6, 132.3, 131.4, 131.0, 130.6, 129.2, 127.4, 70.6, 36.2, 27.0. Exact mass ($M+H^+$): calc'd, 223.1083; found, 223.1078.

Synthesis of 46. 1 equivalent (83.8 mg, 0.44 mmol) of *tert*-butyl 3-(aminooxy) propylcarbamate was used to synthesize **45**, as above. Following Boc deprotection and prior to purification, 2 equivalents $(Ac)_2O$ (83.2 μL, 0.88 mmol) and 2.5 equivalents DIEA (191.6 μL, 1.1 mmol) were added. Reaction progress was monitored by analytical HPLC at 254 nm, and the product was purified by preparatory reverse phase HPLC. As above, the E and Z enantiomers were separable, but were recombined to yield 108.3 mg (93% yield) of the 3-((3-acetamidopropoxyimino)methyl)benzoic acid product **46**. ^1H NMR

(DMSO-d_6): δ 13.14 (s, 1H), 8.33 (s, 1H), 8.18 (t, 1.8 Hz, 1H), 7.95 (app dt, 7.5, 1.5 Hz, 1H), 7.87 (br t, 4.8 Hz, 1H), 7.83 (app dt, 8.3, 1.5 Hz, 1H), 7.54 (app t, 7.8 Hz, 1H), 4.14 (t, 6.5 Hz, 2H), 3.12 (m, 2H), 1.79 (s, 3H), 1.78 (m, 2H). ^{13}C NMR (DMSO-d_6): δ 169.1, 166.8, 148.0, 132.5, 131.3, 130.9, 130.4, 129.2, 127.4, 71.5, 35.4, 28.9, 22.6. Exact mass ($M+H^+$): calc'd, 265.1188; found, 265.1199.

Synthesis of 47. The synthesis and purification of **47** proceeded as described for **45**, but with 4-fluorobenzaldehyde. Yield: 66.8 mg (74%). ^{1}H NMR (DMSO-d_6): δ 8.27 (s, 1H), 7.86 (br s, 3H), 7.66 (m, 2H), 7.26 (m, 2H), 4.17 (t, 6.3 Hz, 2H), 2.90 (m, 2H), 1.94 (m, 2H). ^{13}C NMR (DMSO-d_6): δ 164.0, 162.0, 129.0 (J = 28 Hz), 128.5 (J = 11 Hz), 115.9 (J = 86 Hz), 70.4, 36.2, 27.0. Exact Mass ($M+H^+$): calc'd, 197.1090; found, 197.1091.

Synthesis of 48. The synthesis and purification of **48** proceeded as described for **46**, but with 4-fluorobenzaldehyde. Yield: 103.3 mg (89%). ^{1}H NMR (DMSO-d_6): δ 8.24 (s, 1H), 7.87 (br s, 1H), 7.65 (m, 2H), 7.24 (m, 2H), 4.10 (t, 6.5 Hz, 2H), 3.11 (m, 2H), 1.78 (s, 3H), 1.76 (m, 2H). ^{13}C NMR (DMSO-d_6): δ 169.1, 164.0, 162.0, 129.0 (J = 33 Hz), 128.6 (J = 13 Hz), 115.8 (J = 87.5 Hz), 71.3, 35.5, 28.9, 22.6. Exact Mass ($M+H^+$): calc'd, 239.1196; found, 239.1189.

Determination of DNA Melting Temperature (Tm) values. Melting Temperatures were measured according to a previously published methodology on a Varian Cary 100 spectrophotometer equipped with a thermocontrolled cuvette holder, and quartz cuvettes (1 cm pathlength)[18]. The buffer was an aqueous solution of 10 mM sodium cacodylate, 10 mM KCl, 10 mM $MgCl_2$, and 5 mM $CaCl_2$ at pH 7.0. Oligonucleotide sequences were: 5'-GTGCATACGTGGGC-3' (HRE 14mer top); 5'-GCCCACGTATGCAC-3' (HRE 14mer bottom); 5'-TTGCAGAACAGCAA-3' (ARE 14mer top); and 5'-TTGCTGTTCTGCAA-3' (ARE 14–mer bottom).

Cell Culture Experiments. For cell culture experiments, a polyamide stock solution in DMSO and DNAse/RNAse-free water was prepared by dissolving 5-30 nmol polyamide in DMSO (1-3 μL), followed by addition of DNAse/RNAse-free water to a target concentration

of 50 M. Suspensions were centrifugated to remove undissolved material, and solution concentration determined by UV-vis measurement of a 100× diluted solution at 310 nm (ε = 69,360 M^{-1} cm^{-1} for eight-ring hairpin polyamides.) The DMSO concentration of cell media solutions was kept below 0.1%, and a DMSO control was included in quantitative real-time RT-PCR (see below).[17] Isotherms were generated using the following modified Hill equation: $Y = m_1 + (m_2 - m_1) / (1 + (m_0 / m_3))$; $m_1 = 100$, $m_2 = 5000$, $m_3 = 5e^{-7}$.

Measurement of Cell Viability in U251 and LNCaP Cells. U251 and LNCaP cells were maintained as previously described.[8, 14] For the growth inhibition assay, cells were plated in 96-well plates in 0.2 mL at 10-15 x 10^2 cells per well (15-20 x 10^3 cells/mL). After 24 hours (U251) or 48 hours (LNCaP), 150 μL of media was removed and replaced with 50 μL of 2x (polyamide concentration) cell media solutions. After 48 hours, the media was replaced with 100 μL fresh media, and cells were allowed to recover for 24 hrs before addition of 10 μL WST-1 reagent (Roche) to each well. Cells were incubated for 30 minutes, and absorbance at 450 nm measured. Untreated controls and cell-free, media-only controls were included on each plate, and each well corrected for average background absorption of media-only controls before normalizing average absorption for each concentration to untreated controls.

Measurement of Induced Gene Expression in U251 and LNCaP Cells. Measurement of hypoxia-induced VEGF expression in U251 cells and DHT-induced PSA expression in LNCaP cells was as previously described.[8, 14] Measurement of hypoxia-induced VEGF expression in LNCaP cells followed the protocol for DHT-induced PSA expression in LNCaP cells, with the following changes: gene induction was by DFO, and FBS (not charcoal stripped) was used. Primer sequences were as follows: VEGF, L 5'- AGGGCAGAATCATCACGAAG -3', R 5'-GGGTACTCCTGGAAGATGTCC -3'; PSA, L 5'-TCTGCGGCGGTGTTCTG-3', R 5'-GCCGACCCAGCAAGATCA -3'; ß-glucuronidase, L 5'-CTCATTTGGAATTTTGCCGATT-3', R 5'-CCGAGTGAAGATCCCCTTTTTA-3'.

Table 4.3. MALDI-ToF and Purity data for compounds **1**-**44**.

Compound Number	MALDI-ToF: Expected ($M+H^+$); Observed ($M+H^+$)	Purity*	Compound Number	MALDI-ToF Expected (M+H): Observed (M+H):	Purity*
1	1274.49; 1274.51	99.3	**23**	1237.59; 1237.48	95.0
2	1246.50; 1246.81	99.3	**24**	1209.59; 1209.89	95.6
3	1231.49; 1231.77	99.7	**25**	1194.58; 1194.53	100.0
4	1175.43; 1175.61	98.7	**26**	1138.52; 1138.50	99.7
5	1191.42; 1191.38	97.2	**27**	1154.51; 1154.62	96.8
6	1394.52; 1394.46	98.0	**28**	1357.61; 1357.59	98.8
7	1379.50; 1379.72	99.3	**29**	1342.60; 1342.55	99.6
8	1323.44; 1323.52	99.9	**30**	1286.64; 1286.59	99.0
9	1323.44; 1323.44	95.6	**31**	1286.54; 1286.56	96.1
10	1297.44; 1297.48	95.9	**32**	1260.54; 1260.63	95.3
11	1319.42; 1319.52[a]	97.2	**33**	1260.54; 1260.51	96.4
12	1238.58; 1238.51	96.5	**34**	1238.58; 1238.56	99.0
13	1210.59; 1210.76	98.1	**35**	1210.59; 1210.59	98.0
14	1195.58; 1195.57	98.7	**36**	1195.58; 1195.56	99.3
15	1139.51; 1139.49	98.8	**37**	1139.51; 1139.77	95.1
16	1155.51; 1155.83	98.4	**38**	1155.51; 1155.40	97.4
17	1358.60; 1358.66	97.8	**39**	1358.60; 1358.70	95.4
18	1343.59; 1343.76	99.9	**40**	1343.59; 1343.52	100.0
19	1287.53; 1287.56	99.4	**41**	1287.53; 1287.60	98.4
20	1287.53; 1287.73	97.6	**42**	1287.53; 1287.53	95.9
21	1261.53; 1261.87	97.3	**43**	1261.53; 1261.56	98.9
22	1261.53; 1261.51	98.8	**44**	1261.53; 1261.51	96.2

MALDI-ToF data gives calculated exact mass for ($M+H^+$) and observed mass for ($M+H^+$) for polyamides **1**-**44**. * Purity measured by analytical HPLC at 310 nm; purity for oxime-linked compounds **9**-**11**, **20**-**22**, **31**-**33** and **42**-**44** included both E and Z isomers. [a] Mass found [$M+Na^+$], compound and data provided by Dr. Daniel Harki.

Focused Library of Polyamide-Tail Conjugates

The following section contains unpublished data.

The ability to design and implement potential future applications of polyamides in cell culture or whole organisms depends in part on knowledge of the extent of possible modifications to polyamides available, i.e. whether the FITC and its IPA derivative are discrete, singular solutions to the C-terminal tail identity, isolated but not unique solutions, or members of a much more extensive structure space around the C-terminal tail available for biologically active polyamides. The latter case would indicate that biologically active conjugates of polyamide DNA-recognition elements and other function groups are accessible, e.g. conjugates with by DNA intercalators, DNA cross-linking groups, recognition elements for endogenous or exogenous chemical species, or substrate partners for DNA/polyamide-templated reactions.

To this end, in addition to the linker and linkage modifications detailed above, a library of polyamides was synthesized in which the C-terminal tail group was varied and assayed for changes in biological activity. The HRE- and ARE-targeted match and mismatch polyamide cores were selected and polyamide-tail conjugate biological activity was assessed via induced VEGF (U251 and LNCaP cells) and PSA (LNCaP cells) gene expression evaluated by quantitative real-time RT-PCR measurement of gene mRNA levels. The set of tail moieties selected for study are shown in Figure 4.8, and were designed as a structure-activity relationship series in an attempt to ascertain the structural features of the IPA tail responsible for its enhanced biological activity.

Polyamides **49-60** are HRE match polyamides, **61-72** are HRE mismatch polyamides, **73-84** are ARE match polyamides, and **85-96** are ARE mismatch polyamides. With each set of polyamide cores, a series of 13 tail variations was introduced, including the previously described benzoic acid, 3-hydroxybenzoic acid and IPA conjugates (Chapter 2). As discussed previously, these tails had been initially selected to determine whether the

cell uptake and nuclear localization of the original FITC conjugate was due to the presence of an aromatic ring, a phenol, or a benzoic acid group. Upon identification of the IPA tail as the best combination of ease of synthesis and biological activity, it became of interest to determine, if possible, what structural feature of IPA lay at the heart of its positive activity profile, or how tolerant the C-terminal tail group is to modifications.

To examine the effect of moving the carboxylic acid group from the *meta* to the *para* position on the ring relative to the amide linkage, the terephthalic acid tail was selected. -polyamide conjugates were synthesized. Trimesic acid was introduced as a tail group to determine whether the possible role of the carboxylic acid group in the biological activity of FITC- and IPA-conjugates would be enhanced through addition of another carboxylic acid group. The methyl-ester derivative was designed to probe whether the ability of the carboxylic acid to be deprotonated and carry a negative charge was responsible for biological activity by acting as an endogenous buffer group and facilitating polyamide escape from endosomes and/or acidic lysosomes. The amide and nitro aromatic derivatives are similar in shape to the carboxylic acid group, but differ in charge distribution and surface potential. Both the glutaric acid and cyclohexane-1,3-dicarboxylic acid tail conjugates carry a carboxylic acid group, but lack the aromatic phenyl group of the IPA tail. Methylamine conjugates (e.g. **57**) can be protonated to carry an overall positive charge, but lack the carbonyl group of the amide-bearing conjugates (e.g. **53**). The 3-hydroxy benzoic acid tail had demonstrated some activity in earlier studies and was selected for use here for benchmark comparison to the 3-Fluoro and 4-Fluoro benzoic acid derivatives (Chapter 2).

The cell culture results of polyamides bearing these tails in U251 and LNCaP cells are shown in Figures 4.9-4.11. U251 cells were dosed with HRE match and mismatch core compounds at 1 and 0.5 μM, and the βDp and unconjugated triamine tail controls were included. Differences in the biological activity of these new tail derivatives was less pronounced at 0.5 mM than at 1 μM, but less of a disparity in biological activity was seen

between the match and mismatch compounds at 1 mM than at 0.5 μM. This is similar to what was observed for the oxime-linked compounds above (Figure 4.6). Discussion of HRE cores in U251 will focus on data at the 1 μM dose.

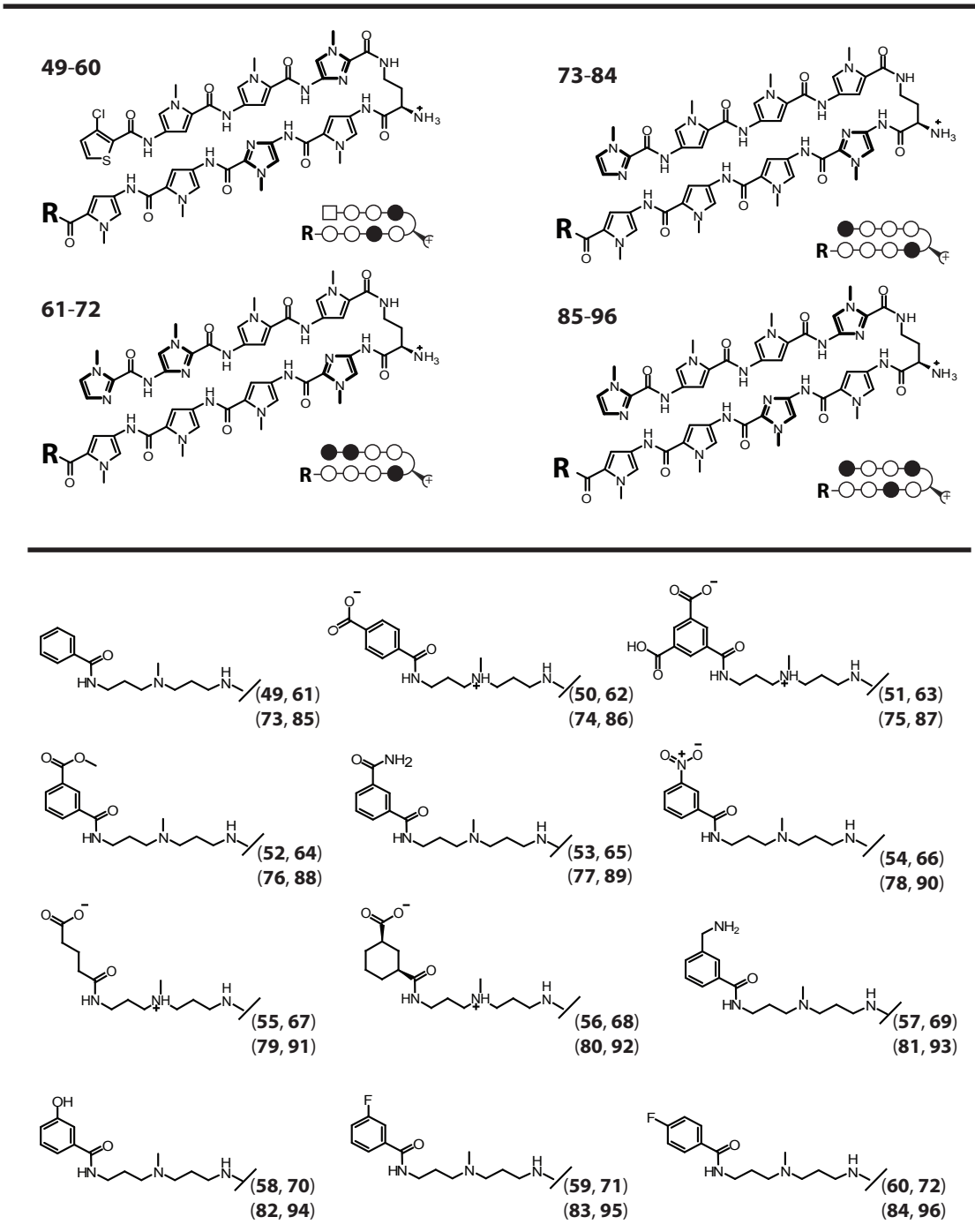

Figure 4.8. Structural representation of polyamide-tail conjugates **49-96**. Shown at top are structural representations of the polyamide heterocycle cores for the VEGF (**49-72**) and PSA (**73-96**) systems. At bottom are shown the structures of the focused library of tails selected for this study.

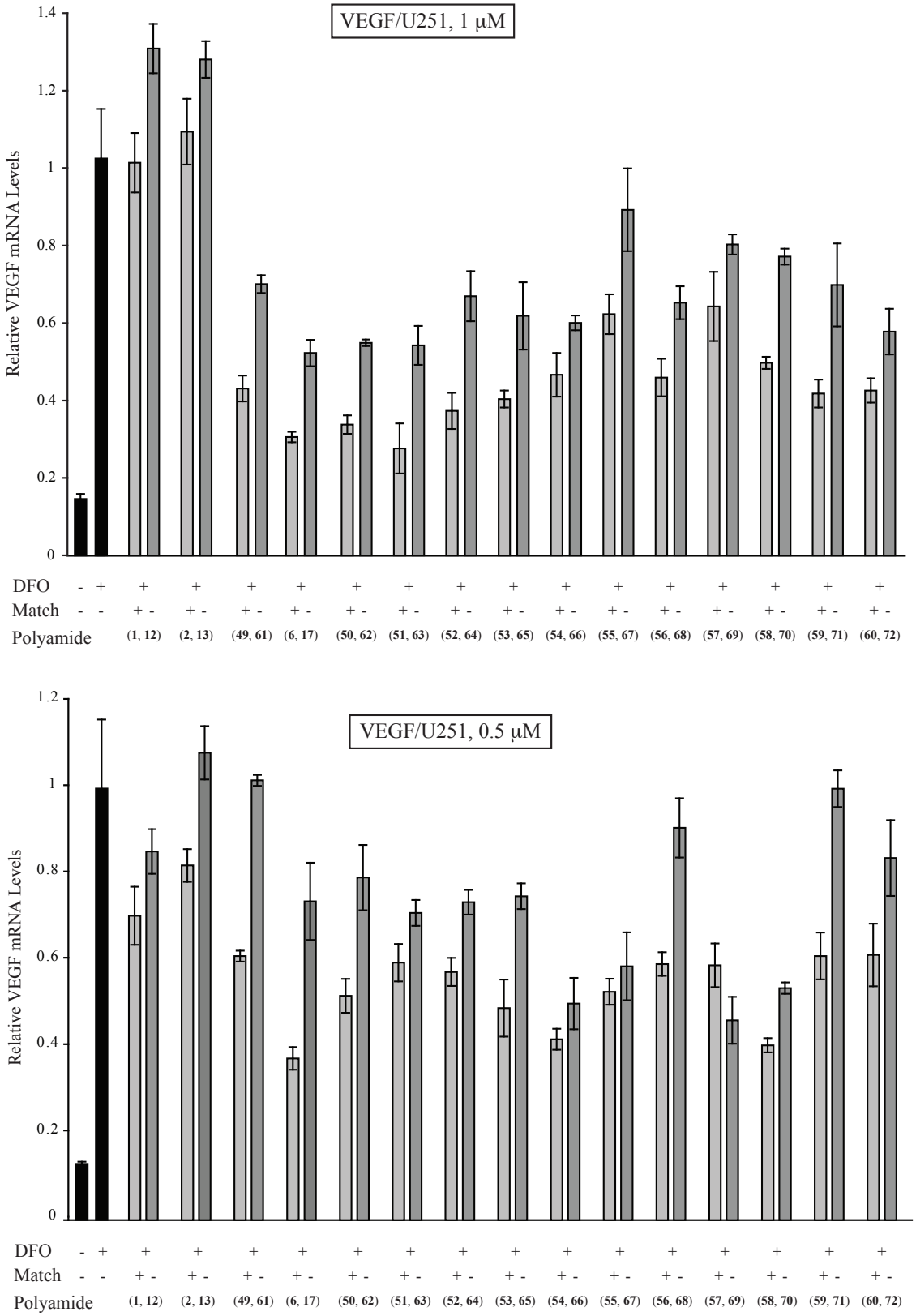

Figure 4.9. Quantitative real-time RT-PCR data in cultured U251 cells induced with DFO and treated with **49**-**72** and controls **1**, **2**, **6**, **12**, **13**, and **17**. U251 cells treated with polyamides at A) 1 μM and B) 0.5 μM.

In U251 cell cultures dosed with polyamides **49**-**72** at 1 μM, the tail identity had an effect on polyamide biological activity, but not in a fashion that facilitated extraction of a set of predictive uptake guidelines. It had been suggested that the presence of the carboxylic acid group in the fluorescein dye acted as an internal buffering group and facilitated polyamide escape from lysosomal acidification. Indeed, moving from the benzoic acid (**49**, **61**) to the IPA (**6**, **17**), terephthalic acid (**50**, **62**) and trimesic acid (**51**, **63**) tails, a slight increase in activity is observed, suggesting that the carboxylic acid is a positive determinant for biological activity. Under the hypothesis suggested above, which implies that activity is predominantly a function of uptake that is facilitated by the acid moiety, it was expected that switching from the IPA tail to the methyl ester would abrogate biological activity. The biological activity of the methyl ester tail derivatives (**52**, **64**) was, however, at best slightly lower than the measured activity of the IPA, terephthalic acid and trimesic acids tails, and was clearly within error of these acid-bearing tail derivatives.

The 3-nitro benzoic acid tail was selected as a means of probing whether the potential negative charge of the carboxylic acid strongly influences polyamides biological activity. Examination of the data in Figure 4.9A reveals a modest decrease in biological activity for the 3-nitro tail derivative compared to the acid-bearing tails, and comparable to the activity of the benzoic acid conjugate (**49**, **61**).

The lack of activity measured in this system for the triamine and βDp tails strongly suggested that the use of an aliphatic linker terminating in an amine group is a negative determinant for polyamide biological activity, and thus that incorporation into the C-terminal tail group of an aromatic phenyl ring rather than the carboxylic acid group is critical to biological activity. In order to evaluate the importance of the aromatic phenyl ring on biological activity, two derivatives lacking the aromatic ring were synthesized and tested: the glutaric acid tail (**55**, **67**), and the 3-carboxycyclohexanoic acid tail (**56**, **68**). The activity of the glutaric acid tail was approximately half that of the IPA tail, and less than that measured for the 3-carboxycyclohexanoic acid tail, which was closer in activity

to the 3-nitro, 3-amide and benzoic acid tails. These results suggest that the presence of a ring is important, and while it need not be an aromatic ring, aromaticity serves further to increase activity in cell culture. The 3-methylamine tail (**57**, **69**) was designed to probe the effect of concurrent removal of the carbonyl group and introduction of a tail capable of carrying a positive charge. This resulted in the most inactive group of the series. Next was a set of three tails comprised of aromatic rings bearing electronegative substituents: 3-hydroxybenzoic acid (**58**, **70**), 3-fluorobenzoic acid (**59**, **71**), and 4-fluorobenzoic acid (**60**, **72**). All three of these derivatives were as active as the benzoic acid tail conjugate.

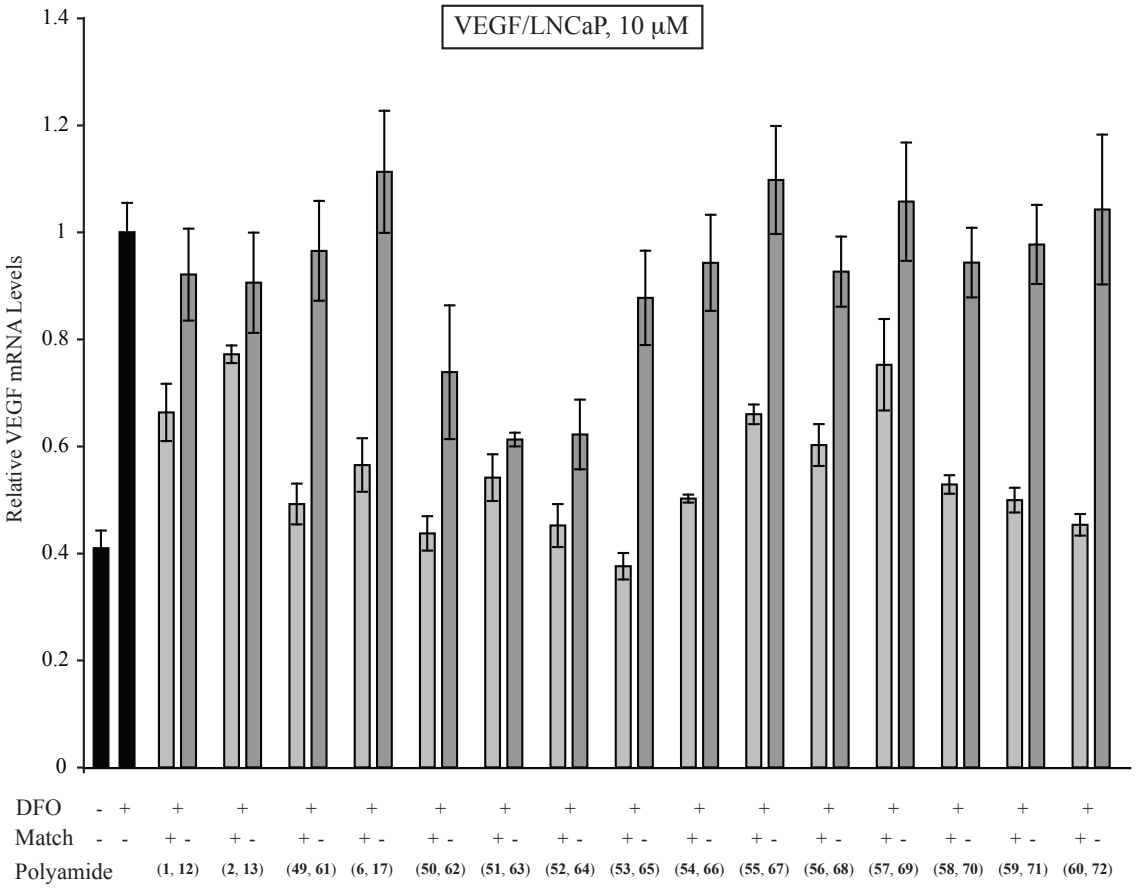

Figure 4.10. Quantitative real-time RT-PCR data in cultured LNCaP cells induced with DFO and treated with **49**-**72** and controls **1**, **2**, **6**, **12**, **13**, and **17**. LNCaP cells treated with polyamides at 10 μM.

To determine whether the trend in activities of these tails was specific to cultured U251 cells, the biological activity of this same series of HRE match and mismatch core tail derivatives was measured in LNCaP cells. The results in LNCaP cells were reasonably

comparable to those in U251 cells. The fold induction of VEGF mRNA was again less in LNCaP cells than in U251. At the concentration tested, there was also a much less significant difference in activity between the control polyamides (**1**, **2**, **12**, **13**) and the IPA tail standard (**6**, **17**) than was measured in the U251 cells at 1 μM. It was encouraging, however, that the data in LNCaP cells did not differ wildly from that in U251 cells, i.e. compounds found to be active in U251 cells were not inactive in LNCaP cells. Further, examination of the LNCaP results (Figure 4.10) shows that there is again appreciable tolerance for modifications to the aromatic ring through introduction of various substituents, while destruction of the aromatic ring or introduction of the methylamine decreased biological activity.

The cell culture results obtained in LNCaP cells for the ARE match and mismatch core series at 10 and 5 μM under inducing (DHT) conditions are shown in Figure 4.11. In contrast to VEGF mRNA induction in LNCaP cells, a 10-fold difference in PSA expression was measured between the uninduced and induced conditions, and a greater degree of variation in biological activity was measured for ARE-core conjugates in LNCaP cells. As for the HRE cores, destruction of the aromatic ring, either in the form of the glutaric acid (**79**, **91**) or 3-carboxylcyclohexanoic acid (**80**, **92**) derivatives resulted in a significant decline in biological activity. The methylamine derivative (**81**, **93**) again showed low levels of biological activity. As with the HRE series in U251 cells, a significant level of tolerance for changes to the ring substituents was observed. With the exception of the glutaric acid, 3-carboxycyclohexanoic acid, methyl amine and trimesic acid tail derivatives, appreciable levels of activity were observed for all other ARE polyamide-tail conjugates.

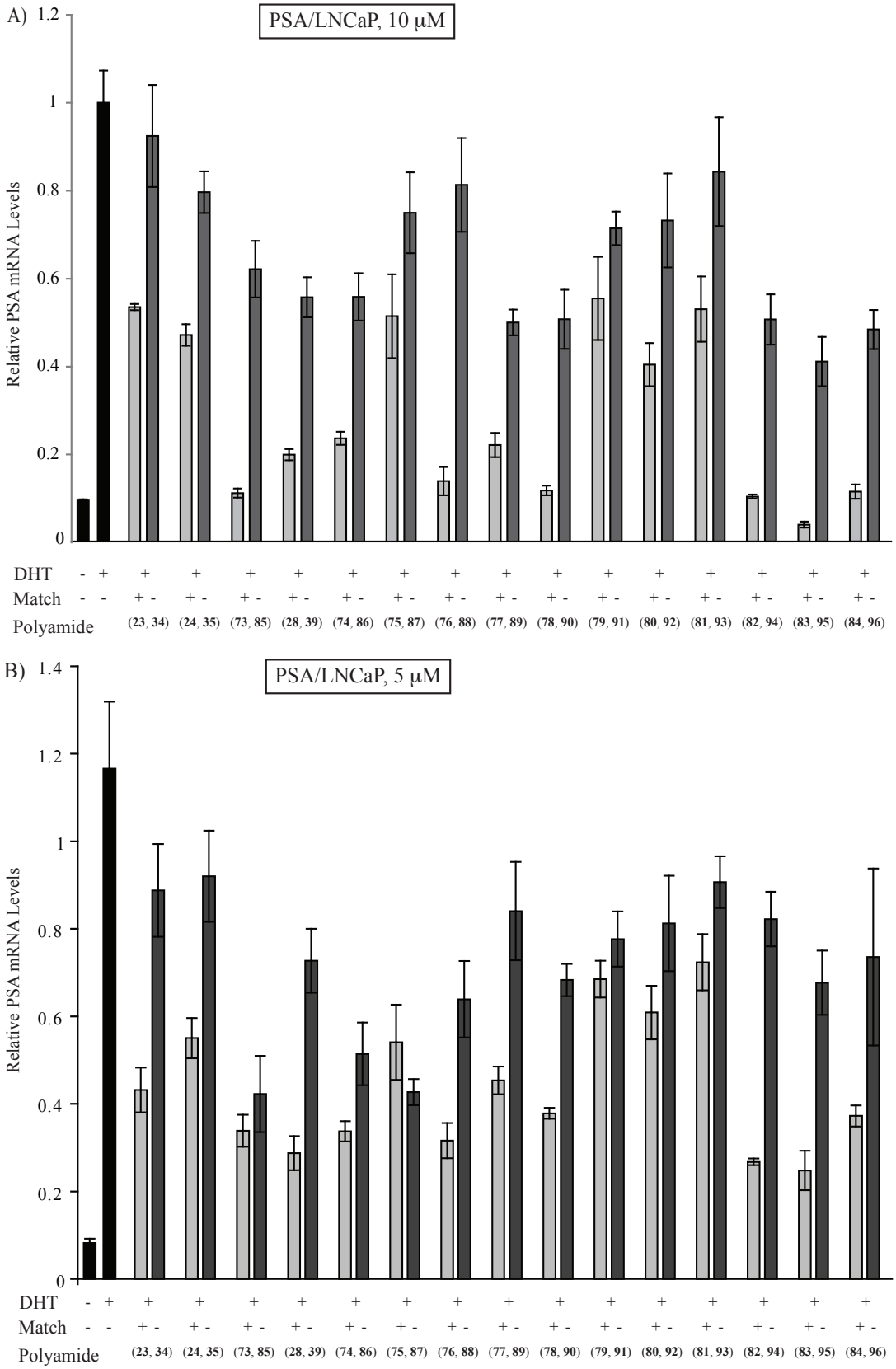

Figure 4.11. Quantitative real-time RT-PCR data in cultured LNCaP cells induced with DHT and treated with **73-96** and controls **23**, **24**, **28**, **34**, **35**, and **39** at A) 10 μM and B) 5 μM.

Although the focused library presented here did not fulfill the primary goal of uncovering structural determinants in the C-terminal tail group of biological activity of polyamides in cell culture, it did provide valuable information. The high level of tolerance for variations in the ring substituents suggests that the IPA tail is not a unique solution to polyamide uptake, but rather that there is an appreciable structure space available for cell-permeable polyamides. In combination with the results presented above for linker and linkage modifications, it appears that the C-terminal portion of polyamides is fungible without endangering compound activity in cell culture. The relative lack of activity measured for polyamides terminating in a βDp tail may reflect the poor activity of eight-ring βDp polyamides rather than polyamides as a compound class. It should be noted at this juncture, however, that other research groups have found success with βDp-terminated two-β-two polyamides.

The results for the ARE-core polyamides in LNCaP were more encouraging than the HRE-core polyamides in either LNCaP or U251 cells. This may reflect lower levels of biological activity of the HRE-match core itself, as the difference in activity of HRE-match and -mismatch congeners is often less than for ARE match/mismatch pairs. In absence of a larger data set of the activity of various cores in numerous cell lines, however, it is difficult to determine whether the HRE-match core is intrinsically less active than pure Im/Py cores. The general concordance between cell lines in the biological activity of this focused library is encouraging, as it suggests that positive hits in one cell line will likely translate into multiple other cell lines. An investigative tool that would aid greatly in efforts to parse whether the modifications being introduced in this study affect biological activity through improved cell uptake, decreased efflux, or another mechanism, is the ability to assay the intranuclear concentration of structurally diverse polyamides. Some efforts have been made in this direction by other researchers in the Dervan group, but have not yet been refined to provide a rapid, reliable intranuclear polyamide concentration assay.

Table 4.4: Tm Data for HRE Cores. Tm DNA only = 64.7 +/- 0.2

5′-G T G C **A T A C G T** G G G C-3′
3′-C A C G **T A T G C A** C C C G-5′

Compound Number	Tm (°C)	ΔTm (°C)	Compound Number	Tm (°C)	ΔTm (°C)
49	76.3 +/- 0.3	15.5	**61**	66.5 +/- 0.3	5.7
50	75.5 +/- 0.3	14.7	**62**	65.0 +/- 0.2	4.2
51	73.6 +/- 0.1	12.8	**63**	64.0 +/- 0.2	3.2
52	76.1 +/- 0.2	15.3	**64**	66.3 +/- 0.2	5.5
53	76.5 +/- 0.3	15.7	**65**	65.9 +/- 0.1	5.1
54	76.3+/- 0.2	15.5	**66**	66.1 +/- 0.1	5.3
55	74.7 +/- 0.2	13.9	**67**	64.3 +/- 0.4	3.5
56	74.7 +/- 0.4	13.9	**68**	64.3 +/- 0.2	3.5
57	78.8 +/- 0.2	18.0	**69**	68.6 +/- 0.4	7.8
58	77.0+/- 0.2	16.1	**70**	66.6 +/- 0.4	5.8
59	76.6 +/- 0.3	15.8	**71**	66.2 +/- 0.2	5.4
60	76.6 +/- 0.3	15.8	**72**	65.9 +/- 0.4	5.1

Oligonucleotide sequences for HRE-core compounds given in Table 4.1; conditions and buffers as for **1**-**44**.

Table 4.5: Tm Data for ARE Cores: Tm DNA only = 60.8 +/- 0.2

5′-T T G C **A G A A C A** G C A A-3′
3′-A A C G **T C T T G T** C G T T-5′

Compound Number	Tm (°C)	ΔTm (°C)	Compound Number	Tm (°C)	ΔTm (°C)
73	76.3 +/- 0.3	15.5	**85**	66.5 +/- 0.3	5.7
74	75.5 +/- 0.3	14.7	**86**	65.0 +/- 0.2	4.2
75	73.6 +/- 0.1	12.8	**87**	64.0 +/- 0.2	3.2
76	76.1 +/- 0.2	15.3	**88**	66.3 +/- 0.2	5.5
77	76.5 +/- 0.3	15.7	**89**	65.9 +/- 0.1	5.1
78	76.3+/- 0.2	15.5	**90**	66.1 +/- 0.1	5.3
79	74.7 +/- 0.2	13.9	**91**	64.3 +/- 0.4	3.5
80	74.7 +/- 0.4	13.9	**92**	64.3 +/- 0.2	3.5
81	78.8 +/- 0.2	18.0	**93**	68.6 +/- 0.4	7.8
82	77.0+/- 0.2	16.1	**94**	66.6 +/- 0.4	5.8
83	76.6 +/- 0.3	15.8	**95**	66.2 +/- 0.2	5.4
84	76.6 +/- 0.3	15.8	**96**	65.9 +/- 0.4	5.1

Oligonucleotide sequences for ARE-core compounds given in Table 4.1; conditions and buffers as for **1**-**44**.

References

1. Brennan, P.; Donev, R.; Hewamana, S., Targeting transcription factors for therapeutic benefit. *Mol Biosyst* **2008,** 4, (9), 909-919.

2. Berg, T., Inhibition of transcription factors with small organic molecules. *Curr Opin Chem Biol* **2008,** 12, (4), 464-471.

3. Dervan, P. B.; Edelson, B. S., Recognition of the DNA minor groove by pyrrole-imidazole polyamides. *Curr Opin Struct Biol* **2003,** 13, (3), 284-299.

4. White, S.; Szewczyk, J. W.; Turner, J. M.; Baird, E. E.; Dervan, P. B., Recognition of the four Watson-Crick base pairs in the DNA minor groove by synthetic ligands. *Nature* **1998,** 391, (6666), 468-471.

5. Kielkopf, C. L.; Baird, E. E.; Dervan, P. B.; Rees, D. C., Structural basis for G.C recognition in the DNA minor groove. *Nat Struct Biol* **1998,** 5, (2), 104-109.

6. Foister, S.; Marques, M. A.; Doss, R. M.; Dervan, P. B., Shape selective recognition of T.A base pairs by hairpin polyamides containing N-terminal 3-methoxy (and 3-chloro) thiophene residues. *Bioorg Med Chem* **2003,** 11, (20), 4333-4340.

7. Hsu, C. F.; Phillips, J. W.; Trauger, J. W.; Farkas, M. E.; Belitsky, J. M.; Heckel, A.; Olenyuk, B. Z.; Puckett, J. W.; Wang, C. C.; Dervan, P. B., Completion of a Programmable DNA-Binding Small Molecule Library. *Tetrahedron* **2007,** 63, (27), 6146-6151.

8. Nickols, N. G.; Jacobs, C. S.; Farkas, M. E.; Dervan, P. B., Improved nuclear localization of DNA-binding polyamides. *Nucleic Acids Res* **2007,** 35, (2), 363-370.

9. Belitsky, J. M.; Leslie, S. J.; Arora, P. S.; Beerman, T. A.; Dervan, P. B., Cellular uptake of N-methylpyrrole/N-methylimidazole polyamide-dye conjugates. *Bioorg Med Chem* **2002,** 10, (10), 3313-3318.

10. Crowley, K. S.; Phillion, D. P.; Woodard, S. S.; Schweitzer, B. A.; Singh, M.; Shabany, H.; Burnette, B.; Hippenmeyer, P.; Heitmeier, M.; Bashkin, J. K., Controlling the intracellular localization of fluorescent polyamide analogues in cultured cells. *Bioorg Med*

Chem Lett **2003,** 13, (9), 1565-1570.

11. Best, T. P.; Edelson, B. S.; Nickols, N. G.; Dervan, P. B., Nuclear localization of pyrrole-imidazole polyamide-fluorescein conjugates in cell culture. *Proc Natl Acad Sci U S A* **2003,** 100, (21), 12063-12068.

12. Edelson, B. S.; Best, T. P.; Olenyuk, B.; Nickols, N. G.; Doss, R. M.; Foister, S.; Heckel, A.; Dervan, P. B., Influence of structural variation on nuclear localization of DNA-binding polyamide-fluorophore conjugates. *Nucleic Acids Res* **2004,** 32, (9), 2802-2818.

13. Olenyuk, B. Z.; Zhang, G. J.; Klco, J. M.; Nickols, N. G.; Kaelin, W. G., Jr.; Dervan, P. B., Inhibition of vascular endothelial growth factor with a sequence-specific hypoxia response element antagonist. *Proc Natl Acad Sci U S A* **2004,** 101, (48), 16768-16773.

14. Nickols, N. G.; Dervan, P. B., Suppression of androgen receptor-mediated gene expression by a sequence-specific DNA-binding polyamide. *Proc Natl Acad Sci U S A* **2007,** 104, (25), 10418-10423.

15. Nickols, N. G.; Jacobs, C. S.; Farkas, M. E.; Dervan, P. B., Modulating hypoxia-inducible transcription by disrupting the HIF-1-DNA interface. *ACS Chem Biol* **2007,** 2, (8), 561-571.

16. Harki, D. A.; Satyamurthy, N.; Stout, D. B.; Phelps, M. E.; Dervan, P. B., In vivo imaging of pyrrole-imidazole polyamides with positron emission tomography. *Proc Natl Acad Sci U S A* **2008,** 105, (35), 13039-13044.

17. Tjernberg, A.; Markova, N.; Griffiths, W. J.; Hallen, D., DMSO-related effects in protein characterization. *J Biomol Screen* **2006,** 11, (2), 131-137.

18. Dose, C.; Farkas, M. E.; Chenoweth, D. M.; Dervan, P. B., Next generation hairpin polyamides with (R)-3,4-diaminobutyric acid turn unit. *J Am Chem Soc* **2008,** 130, (21), 6859-6866.

19. Kalia, J.; Raines, R. T., Hydrolytic stability of hydrazones and oximes. *Angew Chem Int Ed Engl* **2008,** 47, (39), 7523-7526.

20. Juliano, R. L.; Ling, V., A surface glycoprotein modulating drug permeability in

Chinese hamster ovary cell mutants. *Biochim Biophys Acta* **1976,** 455, (1), 152-162.

21. Ueda, K.; Cardarelli, C.; Gottesman, M. M.; Pastan, I., Expression of a full-length cDNA for the human "MDR1" gene confers resistance to colchicine, doxorubicin, and vinblastine. *Proc Natl Acad Sci U S A* **1987,** 84, (9), 3004-3008.

22. Belitsky, J. M.; Nguyen, D. H.; Wurtz, N. R.; Dervan, P. B., Solid-phase synthesis of DNA binding polyamides on oxime resin. *Bioorg Med Chem* **2002,** 10, (8), 2767-2774.

23. Baird, E. E.; Dervan, P.B., Solid Phase Synthesis of polyamides containing imidazole and pyrrole amino acids. *J Am Chem Soc* **1996,** 118, 6141-6146.

24. Salisbury, C. M.; Maly, D. J.; Ellman, J. A., Peptide Microarrays for the Determination of Protease Substrate Specificity *J Am Chem Soc* **2002,** 124, 14868-14870.

25. Wallace, E.; Hurley, B.; Yang, H.; Lyssikatos, J.; Blake, J.; Marlow, A. Heterocyclic inhibitors of MEK and methods of use thereof., US Patent Application 20050054701 A1, 2005.